Soil osmotic potential and its effect on vapor flow from a pervaporative irrigation membrane

Soil Osmotic Potential and Its Effect on Vapor Flow from a Pervaporative Irrigation Membrane

Lindsay C. Todman[1]; Anaïs Chhang[2]; Hannah J. Riordan[3]; Dawn Brooks[4]; Adrian P. Butler[5]; and Michael R. Templeton[6]

Abstract: Pervaporative irrigation is a membrane technology that can be used for desalination and subsurface irrigation simultaneously. To irrigate, the tube-shaped polymer membrane is buried in soil and filled with water. Because of the membrane transport process, water enters the soil in the vapor phase, drawn across the membrane when the relative humidity in the air-filled pores is low. Soils are typically humid environments; however, the presence of hygroscopic compounds such as fertilizers decreases the humidity. For example, at 20°C the humidity in air in equilibrium above a saturated ammonium nitrate solution is 63%. Here, experiments showed that the presence of fertilizers in sand increased the water flux across the membrane by an order of magnitude. An expression for vapor sorption into sand containing different hygroscopic compounds was developed and combined with a model of vapor and liquid flow in soil. The success of the model in simulating experimental results suggests that the proposed mechanism, adsorption of moisture from the vapor phase by hygroscopic compounds, explains the observed increase in the flux from the irrigation system. **DOI: 10.1061/(ASCE)EE.1943-7870.0001379.**

Introduction

Pervaporative irrigation is a promising subsurface irrigation technology that can be used to desalinate water as it is distributed through soil (Quiñones-Bolaños and Zhou 2006; Sule et al. 2013; Muthu and Brant 2015). The technology consists of a semipermeable, nonporous, and hydrophilic polymer membrane, formed into a tube, across which water transport occurs by the process of pervaporation. During irrigation, the pervaporative tube is filled with (saline) water and buried in the soil. If the surrounding soil is dry, a chemical potential gradient across the membrane draws water from inside the tube into the soil, while salt is retained in the tube (Quiñones-Bolaños and Zhou 2006; Muthu and Brant 2015). Notably, during transport water sorbs into the membrane and can only desorb by evaporating; thus water enters the soil in the vapor phase and the water vapor pressure in the soil affects the flux across the membrane. As such, during pervaporative irrigation, soil moisture conditions are the driving force for the process; they provide a feedback mechanism between the crop water uptake and the irrigation flux (i.e., irrigation on demand). Pervaporative irrigation therefore offers passive, low-energy desalinization and enables the use of saline water sources for irrigation without the risk of soil salinization, which would otherwise be a concern. Additionally, the system offers the benefit of autonomous scheduling of water provision to plants. From a scientific perspective, experiments with these membranes also provide a rare opportunity to observe a subsurface flux of water vapor into soil without the addition of heat.

In the field, enough tube must be buried beneath the crop to provide sufficient surface area and hence sufficient water. It would therefore be useful to be able to predict the irrigation flux from the membrane in field conditions and thus estimate the appropriate surface area of the membrane. In other applications of pervaporation, the flux across the membrane is generally controlled directly by maintaining favorable conditions at the downstream edge of the membrane (e.g., Néel 1995). For pervaporative irrigation, however, the conditions at the downstream edge of the membrane are those in the soil pores and are thus affected by the soil moisture conditions, which are in turn affected by the environmental conditions. Working toward the aim of predicting performance in the field, initial models simulate the flux across the pervaporative membrane in bare soils in controlled laboratory conditions (Quiñones-Bolaños and Zhou 2006; Todman et al. 2013a). Results from these models and supporting experimental work have indicated that, in bare soil without plants, the high humidity of the soil environment limits the flux from the membrane (Todman et al. 2013a, b). However, hygroscopic compounds such as fertilizers present in the soil would absorb moisture from the air-filled pores. The equilibrium relative humidity in the air around the resulting salt solution then depends on the osmotic properties of the salt, as the liquid surface effectively forms a semipermeable membrane across which only water can pass. Thus, this decrease in relative humidity should increase the flux from the irrigation membrane. Indeed, the addition of 16 g/kg

[1]Postdoctoral Research Associate, Civil and Environmental Engineering Dept., Imperial College London, South Kensington, London SW7 2AZ, UK; presently, Lecturer in Agricultural Modeling, School of Agriculture, Policy and Development, Univ. of Reading, Reading, Berkshire RG6 6AH, UK (corresponding author). Email: l.todman@reading.ac.uk

[2]M.Sc. Student, Civil and Environmental Engineering Dept., Imperial College London, South Kensington, London SW7 2AZ, UK. Email: anais.chhang@gmail.com

[3]M.Eng. Student, Civil and Environmental Engineering Dept., Imperial College London, South Kensington, London SW7 2AZ, UK. Email: riordan.hannah11@gmail.com

[4]M.Sci. Student, Dept. of Earth Science and Engineering, Imperial College London, South Kensington, London SW7 2AZ, UK. Email: dawn.brooks10@alumni.imperial.ac.uk

[5]Reader in Subsurface Hydrology, Civil and Environmental Engineering Dept., Imperial College London, South Kensington, London SW7 2AZ, UK. Email: a.butler@imperial.ac.uk

[6]Reader in Public Health Engineering, Civil and Environmental Engineering Dept., Imperial College London, South Kensington, London SW7 2AZ, UK. Email: m.templeton@imperial.ac.uk

Note. This manuscript was submitted on May 2, 2017; approved on December 8, 2017; published online on April 30, 2018. Discussion period open until September 30, 2018; separate discussions must be submitted for individual papers. This paper is part of the ***Journal of Environmental Engineering***, © ASCE, ISSN 0733-9372.

of sodium chloride to silica sand increased the flux across the membrane by an order of magnitude compared to clean sand (Todman et al. 2013b).

Pervaporative irrigation systems are of particular interest for irrigation in arid regions, including desert conditions. In these conditions, the ability to make use of low-quality water and to provide water in response to the soil moisture conditions would be particularly valuable. In many arid regions, soils are saline, as the net evaporation from the soil draws salts into the surface layers. Thus, salts at varying concentrations may be present when pervaporative irrigation systems are used in the field. Additionally, when burying the pervaporative tube in desert sand, fertilizers may be applied in order to provide an initial nutrient source to crops. These compounds are hygroscopic (Adams and Merz 1929) and will therefore also affect the osmotic potential and the relative humidity in the soil. As such, a variety of osmotic compounds could be present in the sand, affecting soil conditions and thus the interaction with the pervaporative membrane.

In this paper, a method was developed to incorporate the effects of different osmotic compounds in sand on the flux of water into the soil. This builds on the model of Todman et al. (2013a); however, here the model was parameterized using measurements of the properties of the osmotic compound itself rather than measurements of this osmotic compound in the soil, as was done previously. As such, the approach reduces the need for additional measurements to simulate the effect of different compounds, instead making use of literature data on the water adsorption by the salt where available. Here, three alternative expressions of the soil water retention characteristic curve (SWRC) were considered, focusing on their performance in dry conditions. The effect of osmotic compounds on this curve was then modeled based on knowledge of the osmotic potential of the compound in water. These data are available in the literature for many simple compounds (Scatchard et al. 1938; Hamer and Wu 1972) or could alternatively be measured or simulated. This method thus allows the effect of other salts, and different concentrations of salts, to be simulated in the model, without the need to take sorption isotherm measurements for each scenario. Additionally, an expression for liquid film flow in dry soils was added to the model of vapor flow through soil. The model was tested using previous experimental results (Todman et al. 2013a) that were used to calibrate some model parameters and then validated, for the first time, using new results collected to observe how the flux is affected by the presence of different fertilizers.

Methods

Experimental Methods

Three experiments were conducted to quantify the flux from a pervaporative polymer tube into silica sand with added fertilizers. The distribution of particle sizes in the sand was previously published (Todman et al. 2013b) and ranged from 0.1 to 0.48 mm. The added fertilizers were potassium chloride KCl (6.3 $g\,kg^{-1}$ dry sand), ammonium nitrate $(NH_4)(NO_3)$ (9.4 $g\,kg^{-1}$) and urea CH_4N_2O (9.4 $g\,kg^{-1}$). These represent high concentrations in terms of what might be applied annually to a crop; indeed, assuming an even application, this concentration of ammonium nitrate corresponds to an application rate of approximately $10,000\,m^2$ (5,000 kgN/ha). This is more than an order of magnitude higher than what might be applied even at a high application rate to a nitrogen-hungry crop such as wheat. In other words, it would be unlikely that such a concentration would occur in such a large volume of soil; however, it could occur for a smaller volume in the immediate vicinity of the membrane, and for the purposes of this experiment it was preferable to use a constant concentration in the soil to avoid salt transport. These experiments supplement data from two published experiments (Todman et al. 2013a), conducted following the same method (i.e., same sand, setup, and packing method) but with different osmotic potentials in the sand. One of these experiments had no osmotic compounds added to the sand, and the other had sodium chloride NaCl (16 $g\,kg^{-1}$).

After being oven dried at 105°C for 24 h, the sand was cooled in a desiccated environment, mixed with granular fertilizer at the appropriate density, and packed (1,600 $kg\,m^{-3}$) into the measurement chamber with the irrigation tube running through the center (Fig. 1). The tube and supply reservoir were then filled with deionized water (the desalination ability of the membrane was not used in these experiments), and the mass of a supply reservoir and the humidity in the enclosed chamber above the soil were monitored. The flux of water into the soil was determined from the change in mass of the supply reservoir and assuming an outer diameter of the tube of 26.2 mm (i.e., neglecting corrugations that gave the tube structural strength). During the experiments, the laboratory temperature was maintained at 21 ± 1°C. As each experiment took 3 months to run, they were not repeated. However, the method was previously shown to be highly repeatable (Todman et al. 2013b), and the only alteration here was to use different osmotic compounds. The tube

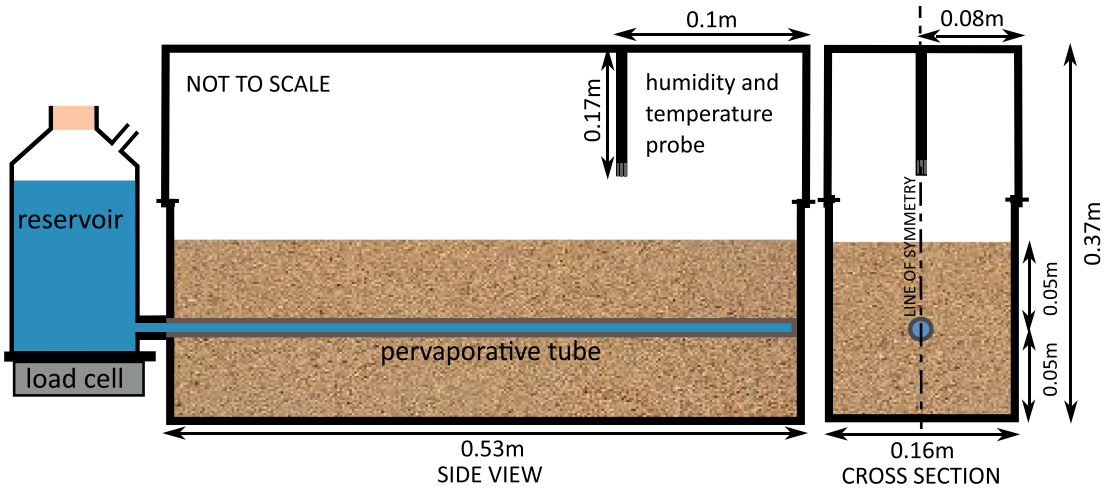

Fig. 1. Experimental setup. (Adapted from Todman et al. 2013b.)

J. Environ. Eng., 2018, 144(7): 04018048

used in these experiments was composed of a nonporous hydrophilic polymer membrane (DuPont de Nemours International, Geneva, Switzerland). The method for packing the sand followed that detailed by Todman et al. (2013a).

Numerical Model

Model of Water Retention and Sorption in Soil

Several mathematical relationships have been developed to describe the SWRC. These originally focused on wetter conditions in which water is primarily held by capillary forces (e.g., Kosugi 1999; van Genuchten 1980). In dry conditions, however, water is primarily held by adsorptive forces. Consequently, models that only represent the capillary range are not suitable for simulations in arid conditions because the inclusion of adsorption affects the simulated vapor flow (Ciocca et al. 2014). To address this, several models that emphasize the SWRC in drier conditions have been developed. Most of these are extensions of models that are frequently used to model the wet range, such as those of Kosugi (1999) and van Genuchten (1980), although some models are new expressions for the entire range of soil moisture contents (e.g., Rossi and Nimmo 1994). Khlosi et al. (2008) compared eight such models, concluding that the model of Khlosi et al. (2006) gave the best fit to the data. Lu et al. (2008) compared three models, including the Khlosi model, and concluded that all three provided adequate representation of their data for eight soils when they were fitted with sufficient data. Subsequently, several additional models have been proposed (Peters 2013; Jensen et al. 2015; Lu 2016), with the Peters model being particularly widely used.

In this study, we compare the ability of three recent models to represent the SWRC observed for the silica sand used in this study. These models are

- Todman et al. (2013a):

$$\theta = \frac{\theta_s - \theta_r}{[1 + (\alpha_1|\psi_m|)^{n_1}]^{m_1}} + \frac{\theta_r}{[1 + (\alpha_2|\psi_m|)^{n_2}]^{m_2}} \tag{1}$$

  where θ_s ($m^3\,m^{-3}$) = saturated water content; θ_r ($m^3\,m^{-3}$) = residual water content; ψ_m (m) = matric potential in the soil; α_1 (m^{-1}) is approximately equal to the air-entry pressure, α_2 (m^{-1}); n_1 and n_2 = additional fitting parameters; and $m = 1 - 1/n$.

- Khlosi et al. (2006):

$$\theta = \frac{1}{2}\left[\theta_s - \theta_a\left(1 - \frac{\ln(|\psi_m|)}{\ln(|\psi_0|)}\right)\right]\operatorname{erfc}\frac{[\ln(\psi_m/\psi_d)]}{\sigma\sqrt{2}} + \theta_a\left(1 - \frac{\ln(|\psi_m|)}{\ln(|\psi_0|)}\right) \tag{2}$$

  where θ_a ($m^3\,m^{-3}$) = curve-fitting parameter representing the water content at $\psi_m = -1$; ψ_0 (m) = water potential at oven dryness (Khlosi et al. suggested $\psi_0 = -10^5$ m); and ψ_d (m) and σ = fitting parameters.

- Peters (2013):

$$\theta = \theta_s\left[w\left(\frac{1}{1 + (\alpha|\psi_m|)^n}\right)^m + (1 - w)X_m\left(1 - \frac{\ln(1 + \psi_m/\psi_a)}{\ln(1 + \psi_0/\psi_a)}\right)\right] \tag{3}$$

  with

$$X_m = \left(1 - \frac{\ln(2)}{\ln(1 + \psi_0/\psi_a)}\right)^{-1}$$

  where w = weighing factor between adsorptive and capillary saturation subjected to $0 \le w \le 1$; α (m^{-1}) = approximate air-entry pressure; n = additional fitting parameter; $m = 1 - 1/n$; and $\psi_a = -\alpha^{-1}$. As in the Khlosi expression, ψ_0 (m) is the matric potential associated with the water content at oven dryness. This expression is slightly modified compared to that of Peters (2013) to avoid a discontinuity in the gradient of the expression that, if used within the numerical model of water flow through soil detailed below, would slow down the numerical solver. In all three expressions, the first term represents the capillary water in the soil; the Khlosi model builds on the Kosugi (1999) model of water retention in this wetter range, whereas the other two models use the van Genuchten (1980) model.

Adsorption of water into soil, which can be represented as the relationship between the water content and the equilibrium relative humidity in the soil (the sorption isotherm), is affected by the presence of added osmotic compounds. Assuming that the matric potential in the soil as a function of the liquid water content is unchanged, the SWRC remains the same despite the presence of a compound. The osmotic potential, however, is increased by the compound and this also affects the equilibrium relative humidity in the air-filled pore space, which can be modeled as (Marshall et al. 1996, p. 71)

$$h = \frac{c_v}{c_{v,\text{sat}}} = \exp\left(\frac{m_w g(\psi_m + \psi_\pi)}{RT}\right) \tag{4}$$

where h = relative humidity; c_v ($mol\,m^{-3}$) = vapor concentration of water in the air in the soil pores; $c_{v,\text{sat}}$ ($mol\,m^{-3}$) = saturated vapor concentration of water; m_w ($kg\,mol^{-1}$) = molar mass of water; g ($m\,s^{-2}$) = acceleration due to gravity; ψ_m (m) = matric potential of the liquid water in the soil; ψ_π (m) = osmotic potential; R ($m^2\,kg\,s^{-2}\,mol^{-1}\,K^{-1}$) = universal gas constant; and T (K) = temperature (21°C for the experiments reported here). In silica sand with no added osmotic compounds, the osmotic potential is negligible, and the sorption isotherm (soil moisture content θ as a function of the relative humidity h) is therefore defined by the SWRC [Eqs. (1), (2), or (3)] and Eq. (4).

Model of Osmotic Potential in Soil

When salts are present in the sand, the osmotic potential can also be quantified. Todman et al. (2013a) measured the water adsorption into sand with added NaCl and used these data to develop an empirical relationship to describe the osmotic potential as a function of the matric potential

$$\psi_\pi = \frac{d_1}{[1 + (\alpha_\pi|\psi_m|)^{n_\pi}]^{m_\pi}} - d_2 \tag{5}$$

where d_2 (m) = osmotic potential of the saturated salt solution; d_1 (m) relates to the maximum osmotic potential in the soil ($d_1 - d_2$, i.e., the smallest absolute value), which depends on the characteristics of the salt, the concentration of salt in the soil, and the volume of pore space in the soil; α_π (m^{-1}) and n_π = shape parameters; and $m_\pi = 1 - 1/n_\pi$. However, if the bulk density of the compound and the water content of the sand are known, the concentration of the solution in the soil is known and the osmotic potential can be inferred. The relationship between osmotic potential and the concentration of a compound in water can be measured experimentally (Hamer and Wu 1972; Scatchard et al. 1938) or estimated using theoretical approaches (Grattoni et al. 2007). When measured, this relationship is often characterized by quantifying the osmotic coefficient (ϕ) at various salt concentrations. Once this coefficient is known, the osmotic potential

can be estimated for any salt concentration by rearranging the Morse equation (Grattoni et al. 2007) to give

$$\psi_\pi = -\frac{\phi(c_{sw}) i c_{sw} RT}{\rho_w g} \tag{6}$$

where c_{sw} (mol m^{-3}) = concentration of the salt in water; i = van 't Hoff factor (i.e., the number of ions present in the molecule, e.g., $i = 2$ for NaCl); and ρ_w (kg m^{-3}) = density of water. Assuming that the dry salt is distributed evenly throughout the soil, the salt concentration in unsaturated solutions can be calculated from a mass balance

$$\theta c_{sw} = c_{sb} \tag{7}$$

where c_{sb} (mol m^{-3}) = bulk concentration of salt in the soil, calculated from the packing density. Because the water content in the soil cannot increase above the saturated water content ($\theta \le \theta_s$), c_{sb}/θ_s is the lowest salt concentration that can occur in the soil water. At low water contents, however, the salt solution will be saturated as follows:

$$c_{sw} = \min(c_{sw,\text{sat}}, c_{sb}/\theta) \tag{8}$$

The relationship between the matric and osmotic potentials can then be calculated using Eq. (6) and a SWRC [Eqs. (1)–(3)]. Here, as the data for osmotic potential were available for a number of discrete points, the relationship between matric and osmotic potentials at these points was calculated and used as data to fit the four parameters for the continuous expression in Eq. (5). The temperature was assumed to remain constant both temporally and spatially as the laboratory temperature was controlled throughout the experiments.

Model of Water Transport in Soil

Transport of water from the membrane and through the soil was modeled in the vapor and liquid phases following the work of Todman et al. (2013a), with the addition of an expression for film flow (Peters 2013). The modeling assumptions are that

- Water transport occurred in the liquid and vapor phases and these two phases were in equilibrium.
- Flows due to temperature effects were negligible.
- Osmotic compounds were distributed evenly throughout the soil and did not move throughout the experiment. This is unlikely in reality, but simplifies the model considerably, and it was assumed that this was reasonable particularly because the soil water content was initially low. Additionally, in a previous experiment, a wetting front of 4 cm was observed after 10 days (Todman et al. 2013b); thus salts were unlikely to move far.

The model uses a two-dimensional (2D) finite-volume method for a cross section of the experiment. A mesh of finite-volume cells was generated to cover half of the cross section (e.g., Todman et al. 2013a), up to a line of symmetry through the middle of the box. All the edges of the box and the line of symmetry were simulated as no-flow boundaries, and the boundary at the edge of the membrane in contact with the soil was simulated as a 100%-relative-humidity surface. This means that water transport from the inner to the outer edge of the membrane was not modeled explicitly. Instead, the flux across the membrane into the soil was determined by Fick's law and depends on the humidity in the air-filled soil pores. The assumption of 100% humidity at the membrane is reasonable because, in the soil close to the membrane, high humidity is likely; thus the transport of water from the membrane into the soil should be the limiting step that regulates the flux. This assumption can be tested by comparison between the simulated and observed experimental flux.

Vapor flow through the soil across the edge of each finite-volume cell was simulated in two dimensions using Fick's law

$$\overrightarrow{q_v} = -m_w D_e(\theta_s - \theta)\nabla c_v \tag{9}$$

where $\overrightarrow{q_v}$ (kg m^{-2} s^{-1}) = mass flux of vapor; m_w (kg mol^{-1}) = molar mass of water; D_e (m^2 s^{-1}) = effective diffusion coefficient; θ (m^3 m^{-3}) = liquid water content of the soil modeled as a function of the soil matric potential using Eq. (4); θ_s (m^3 m^{-3}) = saturated liquid water content of the soil; and c (mol m^{-3}) = concentration of water vapor. Note that $\theta_s - \theta$ quantifies the air-filled porosity. The effective diffusion coefficient $D_e = \tau D_a$, where D_a (m^2 s^{-1}) is the diffusion coefficient for water vapor in air and τ is a parameter used to represent the tortuosity of the pathway for vapor flow through the soil. Although the effective diffusion coefficient is often considered to vary with water content, such changes were not included in this model because it was assumed that the changes in water content are small.

Liquid flow through the soil was simulated using Darcy's law

$$\overrightarrow{q_l} = -\rho K \nabla(\psi_m - z) \tag{10}$$

where $\overrightarrow{q_l}$ (kg m^{-2} s^{-1}) = liquid mass flux; ρ (kg m^{-3}) = density of liquid water; K (m s^{-1}) = hydraulic conductivity; ψ_m (m) = matric potential; and z (m) = depth. The hydraulic conductivity is simulated using (Peters 2013)

$$K = K_s[(1-\omega)K_c + \omega K_f] \tag{11}$$

where K_s (m s^{-1}) = saturated hydraulic conductivity; ω = relative contributions of film flow and capillary flow; the capillary relative conductivity K_c is given by Mualem (1976)

$$\begin{aligned} K_c &= \mathrm{S}_e^{\eta}[1-(1-\mathrm{S}_e^{1/m_1})^{m_1}]^2 \\ \mathrm{S}_e &= [1+(\alpha_1|\psi_m|)^{n_1}]^{-m_1} \end{aligned} \tag{12}$$

and the relative conductivity of the film flow K_f

$$K_f = \begin{cases} (\psi_m/\psi_a)^{-1.5} & \psi_m > \psi_a \\ 1 & \psi_m \le \psi_a \end{cases} \tag{13}$$

The mass of water M_w (kg) within a finite-volume cell, V (m^3), is given by

$$M_w = c m_w V(\theta_s - \theta) + \rho V \theta \tag{14}$$

From continuity, the mass flux into each finite-volume grid cell was equated to the change in mass in that cell; thus

$$\begin{aligned} \int_S (\overrightarrow{q_l} + \overrightarrow{q_v}) \cdot \vec{n} dA = \frac{dM_w}{dt} &= m_w V(\theta_s - \theta)\frac{dc}{d\psi_m}\frac{d\psi_m}{dt} \\ &+ (\rho - c m_w) V \frac{d\theta}{d\psi_m}\frac{d\psi_m}{dt} \end{aligned} \tag{15}$$

where A (m^2) = area; S = surface around a finite-volume cell; and $\vec{n}$ = unit vector normal to the surface of the cell.

Rearranging in terms of the change in matric potential

$$\frac{d\psi_m}{dt} = \frac{\int_S (\overrightarrow{q_l} + \overrightarrow{q_v}) \cdot \vec{n} dA}{m_w V(\theta_s - \theta)(dc/d\psi_m) + (\rho - c m_w) V (d\theta/d\psi_m)} \tag{16}$$

where from Eqs. (1) (for the Todman model of SWRC), (4), and (5)

$$\frac{d\theta}{d\psi_m} = -\frac{m_1 n_1(\theta_s-\theta_r)(\alpha_1|\psi_m|)^{n_1}}{\psi_m[1+(\alpha_1|\psi_m|)^{n_1}]^{m_1+1}} - \frac{m_2 n_2(\theta_s-\theta_r)(\alpha_2|\psi_m|)^{n_2}}{\psi_m[1+(\alpha_2|\psi_m|)^{n_2}]^{m_2+1}}$$
$$\frac{dc}{d\psi_m} = c_{sat}\frac{m_w g}{RT}\left(1+\frac{d\psi_\pi}{d\psi_m}\right)\exp\left(\frac{m_w g(\psi_m+\psi_\pi)}{RT}\right)$$
$$\frac{d\psi_\pi}{d\psi_m} = -\frac{m_\pi n_\pi c d_1(\alpha|\psi_m|)^{n_\pi}}{\psi_m(1+(\alpha|\psi_m|)^{n_\pi})^{n_\pi m_\pi+1}} \quad (17)$$

Eq. (16) is then solved simultaneously for each cell in the finite-volume grid using the *MATLAB* function *ode15s* (Shampine and Reichelt 1997).

Parameter Estimation

SWRC parameters in Eqs. (1)–(3) were estimated by fitting to experimental data for the sand without any added salt. Previously, Khlosi et al. (2008) compared SWRC curves using the root-mean-square error (RMSE); however, RMSE is generally considered biased toward larger values (i.e., wetter conditions) and here dry conditions are of particular interest. Thus, here, the SWRC parameters were fitted by minimizing the mean absolute percentage error between the simulated and observed results (Table 1). Parameters for Eq. (5) were obtained for each salt (Table 2) using literature data for the osmotic coefficients of these salts. These osmotic coefficients were used to derive data for the relationship between the osmotic and matric potential in the sand [Eqs. (6)–(8)]. The parameters were then obtained by fitting Eq. (5) to these derived data. Fitting was carried out using the *MATLAB* function *fminsearch*, which uses the Nelder-Mead simplex algorithm (Mathworks 2017). The tortuosity and hydraulic conductivity parameters (τ, K_s, and η) from Todman et al. (2013a) were used, along with other literature values for standard constants (Table 3). These three parameters were previously fitted to the data for the experiments in sand without added salt and with added NaCl. The same two experiments were again used to confirm that these parameter values were still appropriate when combined with the new model of osmotic potential. The initial conditions for each of the experiments are also given in Table 2.

Table 1. Fitted parameter values for SWRC

Parameter	Value
Fitted parameters for Todman SWRC [Eq. (1)]	
θ_s ($m^3\,m^{-3}$)	0.281
θ_r ($m^3\,m^{-3}$)	0.0055
α_1 (m^{-1})	3.56
α_2 (m^{-1})	0.069
n_1	3.88
n_2	1.30
Fitted parameters for Khlosi SWRC [Eq. (2)]	
θ_s ($m^3\,m^{-3}$)	0.259
θ_a ($m^3\,m^{-3}$)	0.0043
ψ_d (m)	−0.350
σ	0.415
Fitted parameters for Peters SWRC [Eq. (3)]	
θ_s ($m^3\,m^{-3}$)	0.258
w	0.978
α (m^{-1})	3.16
n	4.61

Results

Of the three SWRC expressions considered, all provided good representations of the experimental data for the water retention in sand (Fig. 2), with mean percentage errors of 20, 21, and 23% for the Todman [Eq. (1)], Khlosi [Eq. (2)], and Peters [Eq. (3)] models respectively. Differences in the models occurred mainly at matric potentials where data were sparse. Compared to the Todman model, the Peters and Khlosi expressions improved on the shape (i.e., curvature) of the curve in the drier region and these models have also been more widely used. Nevertheless, the Todman expression provided the best fit to the sorption isotherm during wetting and, given the context, was thus used in further simulations in this paper. Simulations using the Peters model are included in the Appendix, and results in comparison to those simulated using the Todman model are discussed below.

The method developed to simulate the sorption of water into sand with added NaCl provided a very good representation of both the critical humidity, above which water adsorption increases greatly, and the magnitude of this adsorption (Fig. 3). The parameters for the osmotic adsorption were identified based on the literature knowledge of the osmotic compounds, rather than by fitting the model to these data as was done in previous work (Todman et al. 2013a). Using these parameters, along with those for the water flow in the soil (τ, K_s, and η), in the model provided a good simulation of both the relative humidity above the soil and the flux into the sand with added sodium chloride (Fig. 4). The timing of the changes in relative humidity above the sand was well simulated, but the magnitude was underestimated for much of the experiment. In the sand with sodium chloride, the addition of film flow in the

Table 3. Water flow in soil parameters for simulation of pervaporative irrigation

Parameter	Value	Literature source
D_a ($m\,s^{-1}$)	2.45×10^{-5}	Bolz and Tuve (1973)
c_{sat} ($mol\,m^{-3}$)	1.01	Lawrence (2005)[a]
τ	1	Todman et al. (2013a)
K_s ($m\,s^{-1}$)	8×10^{-9}	Todman et al. (2013a)
η	0.1	Todman et al. (2013a)
ω	0.01	Peters (2013)

[a]Estimated at 21°C using the Magnus formula described by Lawrence (2005).

Table 2. Initial conditions and parameter values for the model of the osmotic potential using Eq. (5)

Parameter	No added salt	Sodium chloride	Potassium chloride[a]	Urea[b]	Ammonium nitrate[a]
Initial humidity (%)	40	42	42	17	62
$\boldsymbol{d}_1$ (m)	0	3,157	2,149	3,261	5,379
$\boldsymbol{d}_2$ (m)	0	3,924	2,409	3,503	5,677
$\boldsymbol{\alpha_\pi}$ (m^{-1})	N/A	2.7	2.0	1.6	1.4
$\boldsymbol{n_\pi}$	N/A	10.9	7.6	5.4	3.9

[a]Fitted using measurements from Hamer and Wu (1972).
[b]Fitted using measurements from Scatchard et al. (1938).

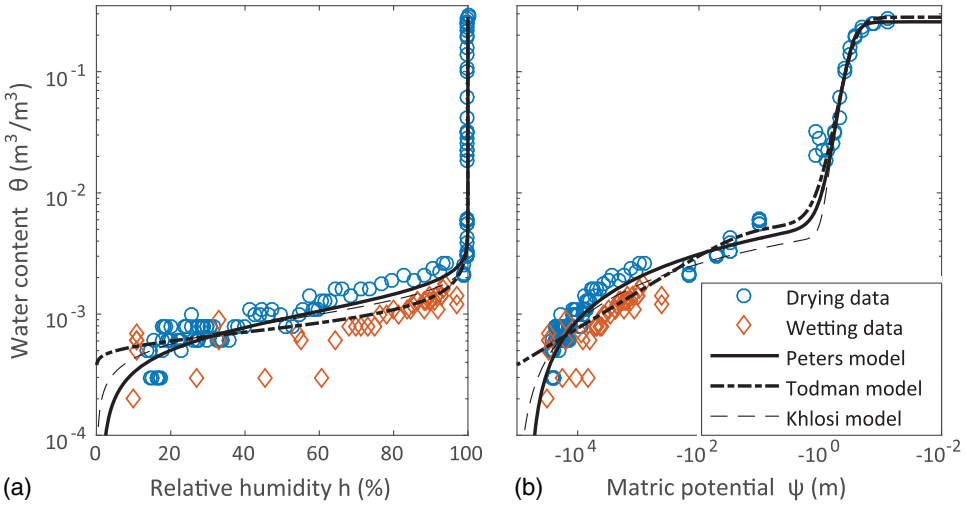

Fig. 2. Observed moisture retention in sand showing the hysteresis in the drying and wetting isotherms and the ability of three nonhysteretic expressions to represent this relationship shown as (a) a moisture sorption isotherm; and (b) the soil water retention characteristic. The two plots show the same data and expressions, and the relative humidity and matric potential are related by Eq. (4), assuming that the osmotic potential is zero. The sorption isotherm highlights the fit of the model in dry conditions.

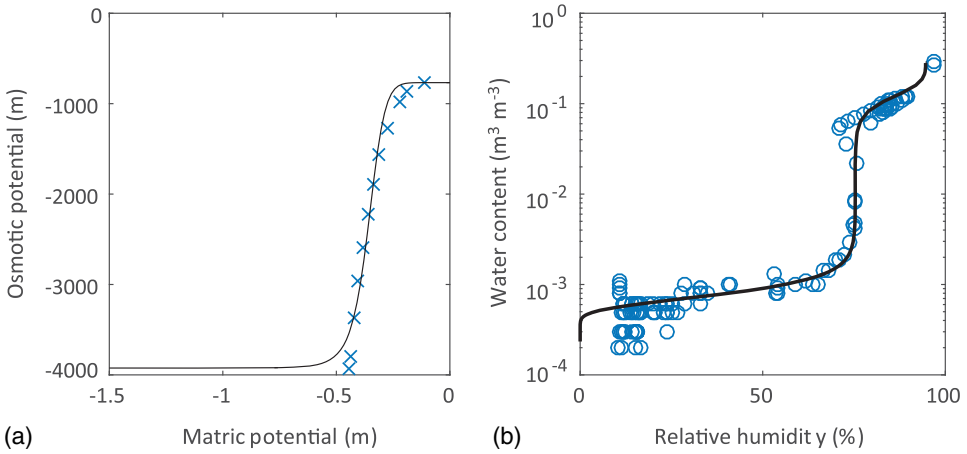

Fig. 3. Effect of 16 kg kg^{-1} sodium chloride on moisture sorption into sand: (a) the fitted relationship between the osmotic and matric potential (line) using data (crosses) derived from literature measurements of the osmotic coefficient of sodium chloride in water (data from Hamer and Wu 1972); and (b) the observed sorption isotherm in saline sand (circles) and the predicted isotherm (line) estimated based on the combined effect of sorption into sand without salt [Fig. 2(a)] and the osmotic effect [Fig. 3(a)].

model improved the flux simulated within the first 20 days [Fig. 4(a)]. In the sand without any added salt, however, including film flow had little effect on the simulated flux as the conditions remained very dry.

When the model was used to predict the results of the three experiments with added fertilizers, the sorption isotherm for the sand with each of the fertilizers added was simulated using literature data for the osmotic coefficient of each compound (Fig. 5). As in the experiments with and without sodium chloride, the timing of the changes in relative humidity was simulated well for all three added fertilizers but the magnitude was underestimated in humid conditions [Figs. 6(b, d, and f)]. The flux into the sand was simulated well in the experiments with urea and ammonium nitrate [Figs. 6(c and e)] but was overestimated in the experiment with potassium chloride [Fig. 6(a)]. Further attention to the relationship between the osmotic and matric potentials in humid conditions may improve this as, in the longer term, the humidity close to the membrane is high. Simulations that used the Peters SWRC (Appendix) showed similar patterns in timing to those with the Todman SWRC, suggesting that the results were not overly sensitive to the choice of SWRC. Notably, the flux into the sand with added potassium chloride was again overestimated. In general, the inclusion of vapor flow and adsorption due to osmotic potential in the model reproduces the large observed increase in flux compared to that observed in sand without added salt.

Discussion

Several models of SWRC for the full range of moisture contents from saturation to oven dryness have been suggested and here only three were compared (Fig. 2). The conclusion, however, was similar to that of Lu et al. (2008), that multiple models can provide adequate fit if sufficient data are available. The data here were

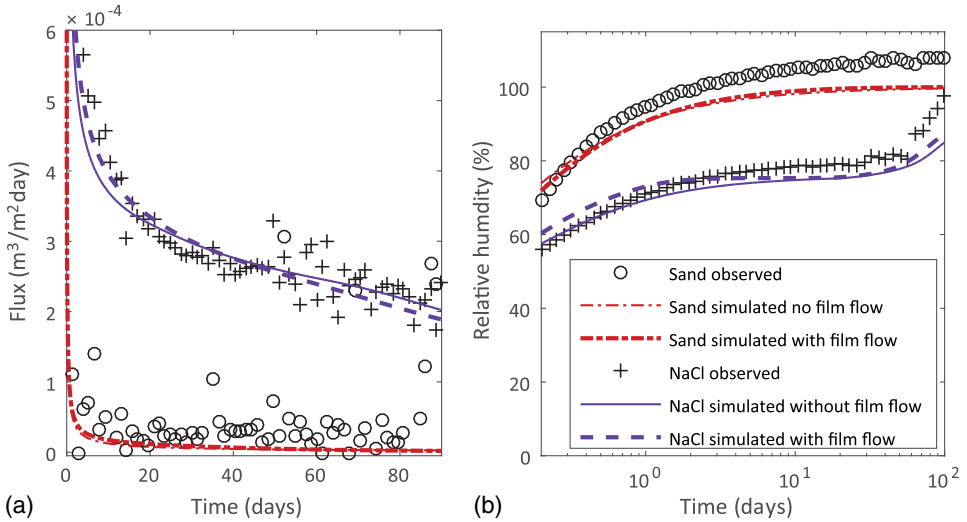

Fig. 4. Observed and simulated: (a) flux from a pervaporative membrane; and (b) relative humidity above the soil in laboratory experiments without any salt (which was used to fit the tortuosity coefficient parameter) and with sodium chloride in the sand (which was used to fit the saturated hydraulic conductivity parameter). The simulations with and without the inclusion of film flow are indistinguishable for the sand without added salt.

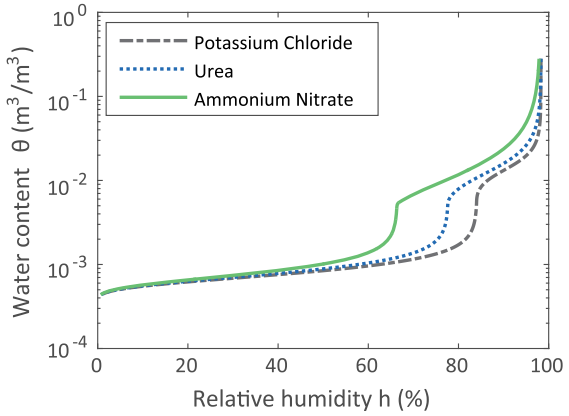

Fig. 5. Simulated moisture sorption isotherms for sand with added fertilizer salts.

biased toward the dry end, with four times as many data points measured using the vapor sorption method than the hanging column and pressure plates. This is unusual because, in other data sets, such as that used for the comparisons made by Khlosi et al. (2008), there are often more data available for the wetter water contents (i.e., those greater than the absorptive range). Thus the performance of SWRC models in the wetter range may dominate the model comparison. Clearly, using one data set is not sufficient to draw conclusions about the performance of the models more generally; however, because of the hysteresis and the fit of the Todman model to the wetting data, that model was particularly relevant in this context.

The method developed here for quantifying the effect of fertilizer compounds on the moisture sorption isotherm was very effective (Fig. 3). This was probably aided by the fact that the compounds were added to a silica sand rather than a soil with finer particles, different mineralogy, and organic matter content, all of which would increase the moisture sorption into the soil without any added hygroscopic compounds (Arthur et al. 2015). The assumption that the sorption due to the salt could be added to that due to the sand may occur because the salt did not interact with the inert sand particles. The method would therefore require testing before being applied for other soil types.

Experimental results showed that, as expected, the addition of any of the fertilizer compounds to the soil increased the flux across the membrane (Fig. 6). The results supported the modeling assumption that the membrane could be simulated as a 100% humidity boundary as the simulated fluxes were similar to those observed experimentally. The effect of osmotic compounds on vapor transport has been much studied within the context of evaporation because the presence of these compounds reduces evaporation (Gran et al. 2011; Nachshon et al. 2011). Part of the mechanism for this reduction is the lower vapor pressure in the soil pores because of the osmotic potential of the soil water solution. In the condensation process observed in the experiments here, it is therefore unsurprising that condensation is increased by the presence of osmotic compounds. Here, the increase in flux was less for the potassium chloride than for either the urea or the ammonium nitrate. This is logical as the equilibrium humidity of a saturated solution of potassium chloride at 20°C is 85% compared to 72 and 63% for saturated solutions of urea and ammonium nitrate respectively. The potential difference across the membrane was therefore initially lower for the potassium chloride experiment. The model, however, should have captured this difference, yet for this simulation only the model overestimated the flux and there is no obvious explanation as to why.

Notably, the model also consistently underestimated the relative humidity in all but the initial day of the experiments (Figs. 4 and 6). This may be due to experimental error, because in conditions close to 100% relative humidity, condensation can form within the probe and increase the observed measurement. In fact, the increase in the measured condensation above 100% in the later stages of the experiment suggests that condensation did occur, but it is not clear when condensation started. Nevertheless, the success of the model in simulating the observed flux and the timing of the humidity increases supports the assumption that the pervaporative membrane can be simulated as a 100% humidity boundary and indicates that the decrease in vapor pressure in the soil because of the presence of osmotic compounds can sufficiently increase the driving force for pervaporation across the membrane, and hence the flux. As with previous work (Todman et al. 2013a, b), the modeling results again

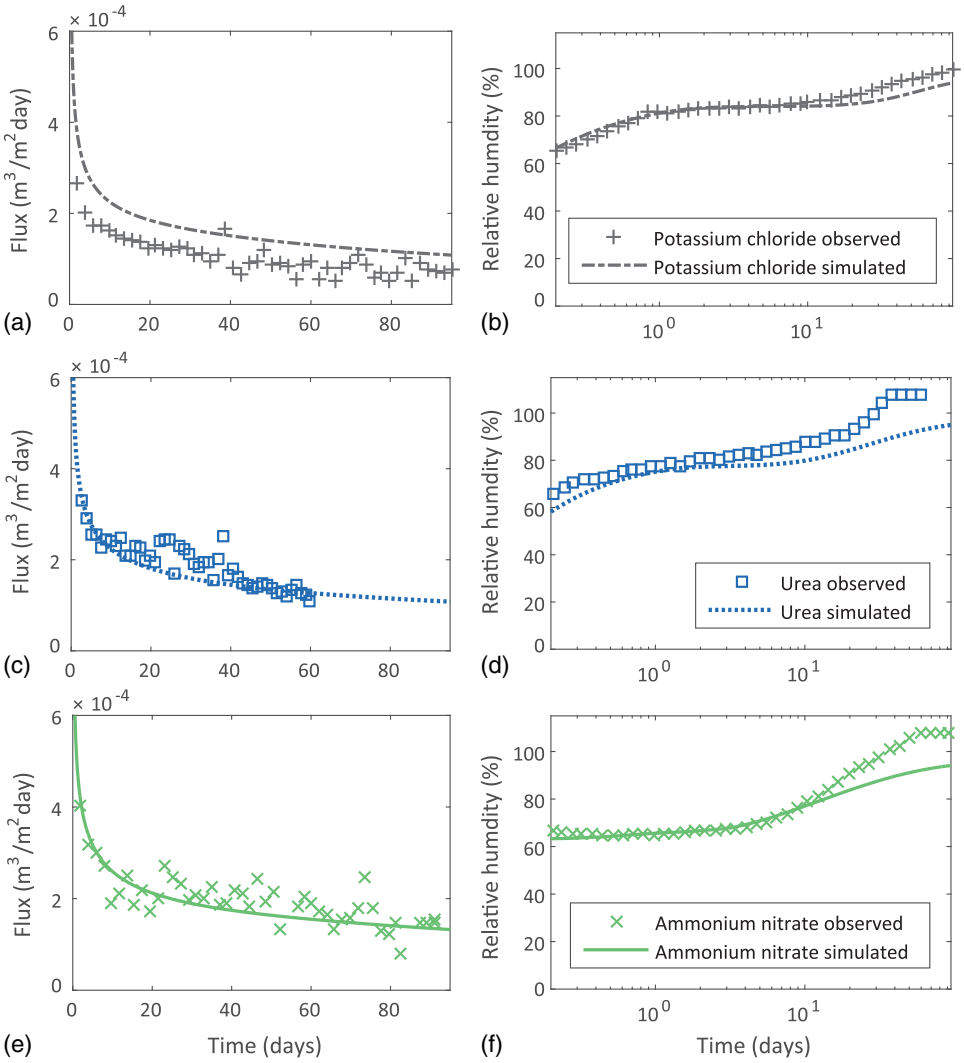

Fig. 6. (a, c, and e) The observed and simulated flux across the pervaporative membrane and (b, d, and f) the observed and simulated relative humidity above the sand into sand with (a and b) added potassium chloride; (c and d) urea; and (e and f) ammonium nitrate.

point toward the importance of soil vapor flows for the performance of pervaporative irrigation membranes.

In field conditions, diurnal temperature variations are also likely to have a significant effect on vapor flows in soil and should be considered in further work. Nevertheless, the behavior of the sorption isotherm of water in sand mixed with an osmotic compound at a given concentration gives an indication of the expected magnitude of the increase in flux because of the presence of that compound. Thus, highly hygroscopic compounds that adsorb large volumes of water at low relative humidity are likely to result in far greater fluxes than those for soils with less hygroscopic compounds. Following the method presented in this paper, these sorption isotherms can now be predicted from knowledge of the sorption isotherm of the sand and the osmotic potential of the relevant compound in water. For simple compounds, such data are available in the literature; however, particularly for more complex compounds or mixtures, measurements could be conducted to estimate this relationship.

The concentration of fertilizers used in the experiments was high. However, the flux increase compared to that for sand without any compounds was more than an order of magnitude. High osmotic potential in the root zone can result in osmotic stress to plants because the potential difference between the soil and roots is reduced, making water uptake more difficult. As such, despite the increase in the water flux into the soil because of the presence of osmotic compounds, this water may not be available to plants. Nevertheless, roots are also known to excrete compounds, often referred to as root exudates, into the soil surrounding the roots (the rhizosphere). Root exudate composition includes hygroscopic sugars and amino acids (Paterson et al. 2007), each of which, individually, would stimulate condensation in the rhizosphere and thus vapor flux toward this region. The osmotic potential in the rhizosphere, however, is likely to be affected also by the interaction of the different solutes that are present (Cochrane and Cochrane 2005). Microorganisms in the rhizosphere will also interact with these root exudates; thus the osmotic potential could vary with time. The large effect of soil osmotic potential observed here suggests that root exudates could be an important means for interaction between plants and pervaporative membranes in soil and should be investigated further.

Conclusions

Previous work using this model (Todman et al. 2013a) relied on parameter values fitted to data collected specifically to measure

the adsorption of water into a sand with an added osmotic compound. The method presented here allows these parameters to be estimated from literature values or independent measurements of the osmotic compounds out of the soil, and it is very effective. This allows the model to be applied much more readily to simulate the effect of different compounds at variable concentrations. Additionally, the success of the model in simulating the results of experiments conducted using different osmotic compounds provides further evidence to support the proposed mechanism simulated in the model—that vapor flow and soil vapor sorption play an important role in the performance of pervaporative irrigation membranes. Along with the new experimental observations in soils with three different fertilizers added, which in all cases showed an order of magnitude increase in flux compared to sand without added fertilizer, this suggests that osmotic compounds in the soil should be considered when evaluating this irrigation approach because of their effect on relative humidity in the soil.

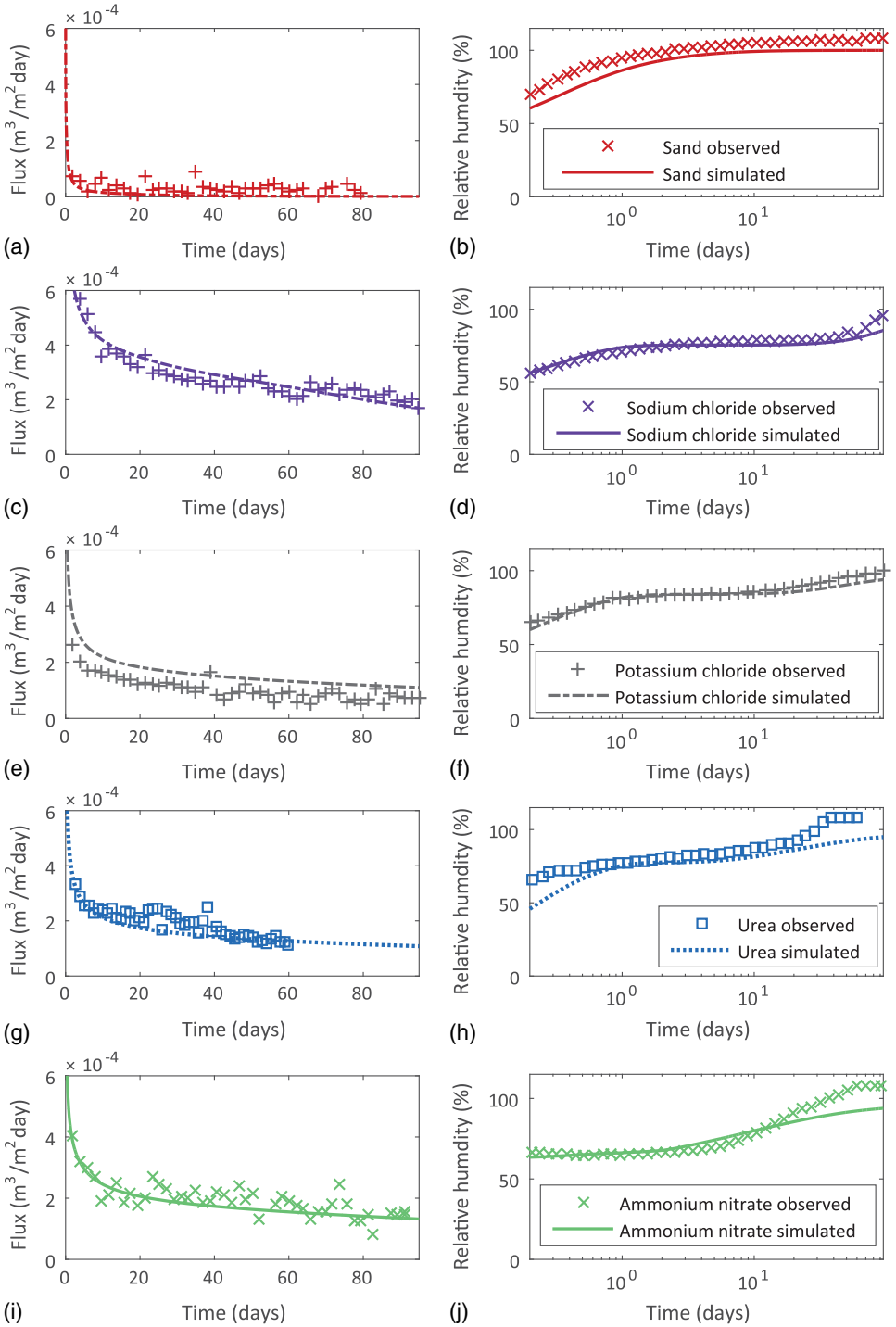

Fig. 7. Water flux and relative humidity simulated using the Peters model of soil water retention [Eq. (3)]. Results are shown for simulations in sand with (a and b) no osmotic compound and for (c–j) the addition of four different added osmotic compounds. Simulated results are compared to those observed experimentally.

Appendix. Model Simulations Using an Alternative Soil Water Retention Curve

To consider the sensitivity of the model to the choice of soil water retention curve (SWRC), the simulations of flux and relative humidity into the sand with different salts were also performed using the Peters (2013) model. The model equations were as described, except for Eq. (17), for which $d\theta/d\psi_m$ was instead calculated by differentiating Eq. (3). These model simulations (Fig. 7) showed similar patterns as those seen using the Todman et al. (2013a) model. More specifically, using the Peters SWRC, the model still simulated the flux well in all cases except the potassium chloride, when the flux was again overestimated. The relative humidity was again overestimated in the later stages of the test.

Acknowledgments

We gratefully acknowledge the EPSRC Imperial College doctoral prize fellowship that supported LCT and the in-kind support of DTI-r Ltd. and DuPont, without which this work would not have been possible. We also thank two anonymous reviewers for their comments and suggestions that helped improve this work.

References

Adams, J. R., and A. R. Merz. 1929. "Hygroscopicity of fertilizer materials and mixtures." *Ind. Eng. Chem.* 21 (4): 305–307. https://doi.org/10.1021/ie50232a003.

Arthur, E., M. Tuller, P. Moldrup, D. K. Jensen, and L. W. De Jonge. 2015. "Prediction of clay content from water vapour sorption isotherms considering hysteresis and soil organic matter content." *Eur. J. Soil Sci.* 66 (1): 206–217. https://doi.org/10.1111/ejss.12191.

Bolz, R. E., and G. L. Tuve. 1973. *Handbook of tables for applied engineering science*. 2nd ed. Boca Raton, FL: CRC Press.

Ciocca, F., I. Lunati, and M. B. Parlange. 2014. "Effects of the water retention curve on evaporation from arid soils." *Geophys. Res. Lett.* 41 (9): 3110–3116. https://doi.org/10.1002/2014GL059827.

Cochrane, T. T., and T. A. Cochrane. 2005. "Osmotic potential properties of solutes common in the soil-plant solution continuum." *Soil Sci.* 170 (6): 433–444. https://doi.org/10.1097/01.ss.0000169916.55850.f3.

Gran, M., J. Carrera, S. Olivella, and M. W. Saaltink. 2011. "Modeling evaporation processes in a saline soil from saturation to oven dry conditions." *Hydrol. Earth Syst. Sci.* 15 (7): 2077–2089. https://doi.org/10.5194/hess-15-2077-2011.

Grattoni, A., M. Merlo, and M. Ferrari. 2007. "Osmotic pressure beyond concentration restrictions." *J. Phys. Chem. B.* 111 (40): 11770–11775. https://doi.org/10.1021/jp075834j.

Hamer, W. J., and Y. C. Wu. 1972. "Osmotic coefficients and mean activity coefficients of uni-univalent electrolytes in water at 25°C." *J. Phys. Chem. Ref. Data.* 1 (4): 1047–1100. https://doi.org/10.1063/1.3253108.

Jensen, D. K., M. Tuller, L. W. de Jonge, E. Arthur, and P. Moldrup. 2015. "A new two-stage approach to predicting the soil water characteristic from saturation to oven-dryness." *J. Hydrol.* 521: 498–507. https://doi.org/10.1016/j.jhydrol.2014.12.018.

Khlosi, M., W. M. Cornelis, A. Douaik, M. T. van Genuchten, and D. Gabriels. 2008. "Performance evaluation of models that describe the soil water retention curve between saturation and oven dryness." *Vadose Zone J.* 7 (1): 87–96. https://doi.org/10.2136/vzj2007.0099.

Khlosi, M., W. M. Cornelis, D. Gabriels, and G. Sin. 2006. "Simple modification to describe the soil water retention curve between saturation and oven dryness." *Water Resour. Res.* 42 (11): W11501. https://doi.org/10.1029/2005WR004699.

Kosugi, K. 1999. "General model for unsaturated hydraulic conductivity for soils with lognormal pore-size distribution." *Soil Sci. Soc. Am. J.* 63 (2): 270. https://doi.org/10.2136/sssaj1999.03615995006300020003x.

Lawrence, M. G. 2005. "The relationship between relative humidity and the dewpoint temperature in moist air: A simple conversion and applications." *Bull. Am. Meteorol. Soc.* 86 (2): 225–233. https://doi.org/10.1175/BAMS-86-2-225.

Lu, N. 2016. "Generalized soil water retention equation for adsorption and capillarity." *J. Geotech. Geoenviron. Eng.* 142 (10): 04016051. https://doi.org/10.1061/(ASCE)GT.1943-5606.0001524.

Lu, S., T. Ren, Y. Gong, and R. Horton. 2008. "Evaluation of three models that describe soil water retention curves from saturation to oven dryness." *Soil Sci. Soc. Am. J.* 72 (6): 1542–1546. https://doi.org/10.2136/sssaj2007.0307N.

Marshall, T. J., J. W. Holmes, and C. W. Rose. 1996. *Soil physics*. 3rd ed. New York: Cambridge University Press.

Mathworks. 2017. "Global optimization toolbox: User's guide (r2017a)." Accessed August 2, 2017. http://www.mathworks.com/help/pdf_doc/optim/optim_tb.pdf.

Mualem, Y. 1976. "A new model for predicting the hydraulic conductivity of unsaturated porous media." *Water Resour. Res.* 12 (3): 513–522. https://doi.org/10.1029/WR012i003p00513.

Muthu, S., and J. A. Brant. 2015. "Interrelationships between flux, membrane properties, and soil water transport in a subsurface pervaporation irrigation system." *Environ. Eng. Sci.* 32 (6): 539–550. https://doi.org/10.1089/ees.2014.0519.

Nachshon, U., N. Weisbrod, M. I. Dragila, and A. Grader. 2011. "Combined evaporation and salt precipitation in homogeneous and heterogeneous porous media." *Water Resour. Res.* 47 (3): W03513. https://doi.org/10.1029/2010WR009677.

Néel, J. 1995. "Pervaporation." In *Membrane separations technology: Principles and applications*. 1st ed., edited by R. D. Noble and S. A. Stern, 143–212. Amsterdam: Elsevier.

Paterson, E., T. Gebbing, C. Abel, A. Sim, and G. Telfer. 2007. "Rhizodeposition shapes rhizosphere microbial community structure in organic soil." *New Phytol.* 173 (3): 600–610. https://doi.org/10.1111/j.1469-8137.2006.01931.x.

Peters, A. 2013. "Simple consistent models for water retention and hydraulic conductivity in the complete moisture range." *Water Resour. Res.* 49 (10): 6765–6780. https://doi.org/10.1002/wrcr.20548.

Quiñones-Bolaños, E., and H. Zhou. 2006. "Modeling water movement and flux from membrane pervaporation systems for wastewater microirrigation." *J. Environ. Eng.* 132 (9): 1011–1018. https://doi.org/10.1061/(ASCE)0733-9372(2006)132:9(1011).

Rossi, C., and J. R. Nimmo. 1994. "Modeling of soil water retention from saturation to oven dryness." *Water Resour. Res.* 30 (3): 701–708. https://doi.org/10.1029/93WR03238.

Scatchard, G., W. J. Hamer, and S. E. Wood. 1938. "Isotonic solutions. I. The chemical potential of water in aqueous solutions of sodium chloride, potassium chloride, sulphuric acid, sucrose, urea and glycerol at 25°C." *J. Am. Chem. Soc.* 60 (12): 3061–3070. https://doi.org/10.1021/ja01279a066.

Shampine, L. F., and M. W. Reichelt. 1997. "The MATLAB ODE suite." *SIAM J. Sci. Comput.* 18 (1): 1–22. https://doi.org/10.1137/S1064827594276424.

Sule, M., J. Jiang, M. Templeton, E. Huth, J. Brant, and T. Bond. 2013. "Salt rejection and water flux through a tubular pervaporative polymer membrane designed for irrigation applications." *Environ. Technol.* 34 (10): 1329–1339. https://doi.org/10.1080/09593330.2012.746736.

Todman, L. C., A. M. Ireson, A. P. Butler, and M. R. Templeton. 2013a. "Modeling vapor flow from a pervaporative irrigation system." *Vadose Zone J.* 12 (4), in press. https://doi.org/10.2136/vzj2013.05.0079.

Todman, L. C., A. M. Ireson, A. P. Butler, and M. R. Templeton. 2013b. "Water vapor transport in soils from a pervaporative irrigation system." *J. Environ. Eng.* 139 (8): 1062–1069. https://doi.org/10.1061/(ASCE)EE.1943-7870.0000715.

van Genuchten, M. T. 1980. "A closed-form equation for predicting the hydraulic conductivity of unsaturated soils." *Soil Sci. Soc. Am. J.* 44 (5): 892–898. https://doi.org/10.2136/sssaj1980.03615995004400050002x.